Geomechanics and Engineering, *Vol. 13, No. 1 (2017) 99-117*
DOI: https://doi.org/10.12989/gae.2017.13.1.099

Rock physics modeling in sand reservoir through well log analysis, Krishna-Godavari basin, India

Dip Kumar Singha [1a] and Rima Chatterjee [*2]

[1] *Department of Geophysics, Institute of Science, Banaras Hindu University, Varanasi 221005, India*
[2] *Department of Applied Geophysics, Indian Institute of Technology (Indian School of Mines), Dhanbad 826004, India*

(*Received May 27, 2016, Revised January 11, 2017, Accepted February 16, 2017*)

Abstract. Rock physics modeling of sandstone reservoir from gas fields of Krishna-Godavari basin represents the link between reservoir parameters and seismic properties. The rock physics diagnostic models such as contact cement, constant cement and friable sand are chosen to characterize reservoir sands of two wells in this basin. Cementation is affected by the grain sorting and cement coating on the surface of the grain. The models show that the reservoir sands in two wells under examination have varying cementation from 2 to more than 6%. Distinct and separate velocity-porosity and elastic moduli-porosity trends are observed for reservoir zones of two wells. A methodology is adopted for generation of Rock Physics Template (RPT) based on fluid replacement modeling for Raghavapuram Shale and Gollapalli Sandstones of Early Cretaceous. The ratio of *P*-wave velocity to *S*-wave velocity (*Vp*/*Vs*) and *P*-impedance template, generated for this above formations is able to detect shale, brine sand and gas sand with varying water saturation and porosity from wells in the Endamuru and Suryaraopeta gas fields having same shallow marine depositional characters. This RPT predicted detection of water and gas sands are matched well with conventional neutron-density cross plot analysis.

Keywords: rock physics model; rock physics template; well log data; Krishna-Godavari Basin; neutron-density cross plot

1. Introduction

Rock physics models relate the link between reservoir parameters such as: porosity, clay content, sorting, lithology, water saturation and seismic properties, namely; ratio of *P*-wave velocity (*Vp*) to S-wave velocity (*Vs*), density and elastic moduli. A study on petrophysics deals with the properties of porous media such as: porosity, permeability, water saturation, fluid identification, resistivity, shaliness particularly in reservoir rock and contained fluids (e.g., Mukerji *et al*. 2001, Sarasty and Stewart 2003, Omudu *et al*. 2008). These properties and their relationship are generally used to identify and assess reservoir rock, source rock and cap rock. Rock physics models are used to estimate seismic properties from the observed petrophysical and reservoir properties (Mavko *et al*. 1998, Samantaray and Gupta 2008, Gray *et al*. 2015). Geological factors such as: reservoir heterogeneity, sorting, digenetic quartz cementation on sandstone, clay content

∗Corresponding author, Professor, E-mail: rima_c_99@yahoo.com
[a] Ph.D., E-mail: dipgeo89@gmail.com; dip28kolktata@gmail.com

http://www.techno-press.org/?journal=gae&subpage=7 ISSN: 2005-307X (Print), 2092-6219 (Online)

and depositional characters control the rock physics and seismic properties Avseth *et al*. (2005, 2009).

Previously, rock physics template (RPT) has been built for specific reservoirs of Cambay basin to guide seismic inversion interpretation results for reservoir characterization and fluids identification purpose (Datta Gupta *et al*. 2012, Chatterjee *et al*. 2013).

Therefore the demonstration of rock physics modeling and generation of RPT of reservoirs in Krishna-Godavari (K-G) basin will be useful for seismic AVO (amplitude variation with offset) inversion and identification of fluid type. Seismic data for the study area is restricted to us. Without seismic data it is difficult to get spatial control over rock physics; hence the case study demonstrating the rock physics modeling is based on well log data only. Well logs namely; gamma ray, resistivity, density, neutron, P-wave and S-wave velocities are considered for reservoir identification from two wells located in Endamuru and Suryaraopeta fields of the basin (Fig. 1). The objectives of this paper are to investigate the use of constant cement model Avseth *et al*. (2000), the contact cement model Dvorkin *et al*. (1994), friable sand model Dvorkin and Nur (1996) and the modified Hashin-Shtrikman (HS) bounds plus the Hertz-Mindlin (HM) theory (Hashin and Shtrikman 1963, Mindlin 1949) for rock physics diagnostic (RPD) modeling. The Gassmann fluid substitution Gassmann (1951a, b) has been applied to predict the dependence of seismic velocity and impedance on pore fluids as bulk modulus changes when pores are filled with different fluids. Rock physics scenarios associated with reservoir zones of K-G basin are performed using fluid replacement modeling to vary porosity, water saturation, and oil density. Therefore, the focus of this paper is aimed to develop a rock physics model of elastic moduli and porosity as well as generation of RPT from the available geological information including petrophysical parameters.

2. Study area

K-G basin is a pericratonic passive basin located at middle part of eastern continental margin of India (ECMI). This basin containing commercial accumulation of hydrocarbon is characterised by horst and graben structures filled with 5-7 km thick pile of sediments of Permian to Recent age (Rao 2001, Gupta 2006).The basin has emerged as one of the frontier areas for future hydrocarbon exploration—after the multi-trillion cubic feet supergiant gas discoveryin the recent years Bastia *et al*. (2010). This basin is subdivided into three sub-basins namely Krishna, west Godavari and east Godavari which are separated by Bapatla and Tanuku horsts respectively (Fig. 1) Sastri *et al*. (1973, 1981). Reservoir rocks in this basin mostly comprise of sandstone, shaly sandstone, siltstone and sandy siltstone, where, the hydrocarbon accumulation is expected in a variety of traps, such as: anticline, fault, unconformity, lens, pinch-outs or their combinations. The non-conventional stratigraphic traps related to channel fills, regional sand pinch-outs and truncations are supposed to be conspicuous hydrocarbon accumulators (Gupta 2006, Shanmugam *et al*. 2009). Two wells namely; KE in Endamuru (END) and KR in Suryaraopeta (SUR) fields are considered for rock physics analysis (Fig. 1).

The well KE has penetrated Kommugudem Formation at depth 2060 m followed by Gollapalli Sandstone and Raghavapuram Shale at the depth interval 1763-2116 m. The other well KR has penetrated Raghavapuram Shale at the depth interval 2023-2429 m. Well log responses such as gamma ray, resistivity, density and neutron porosity logs have been utilized for estimation of petrophysical properties for the hydrocarbon bearing zones of chosen depth intervals (Table 1). Log data such as gamma ray, velocity, P-impedance, *Vp*/*Vs* from these wells in the hydrocarbon

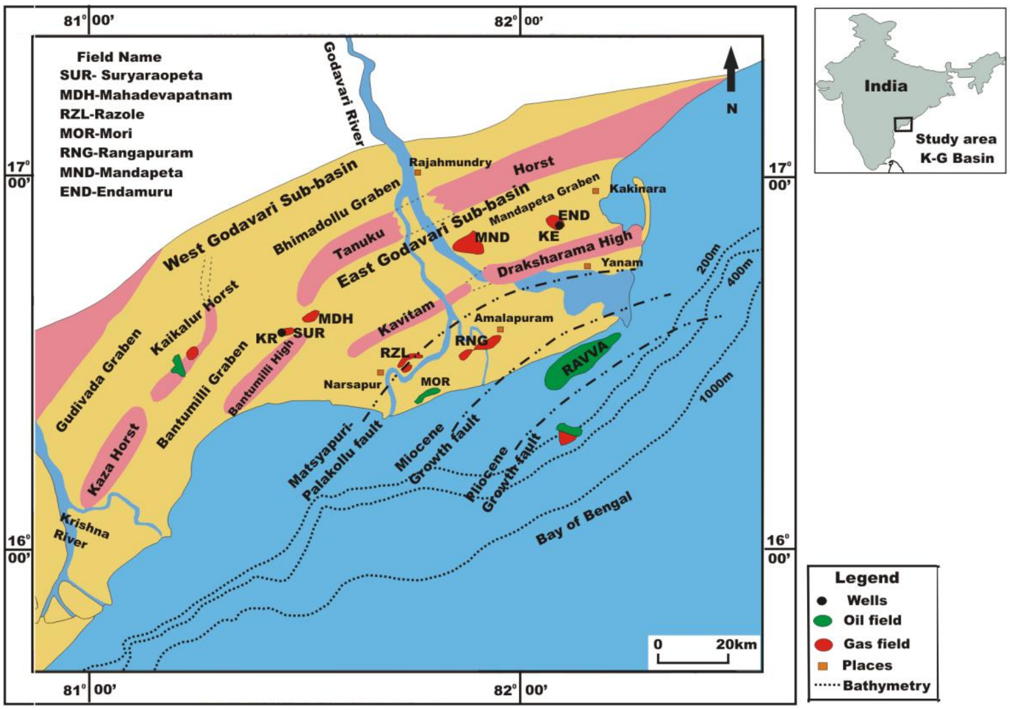

Fig. 1 Showing the tectonic map and well location in the gas fields of Krishna-Godavari basin (after Sastri *et al*. 1973, Rao 2001, Singha and Chatterjee 2014)

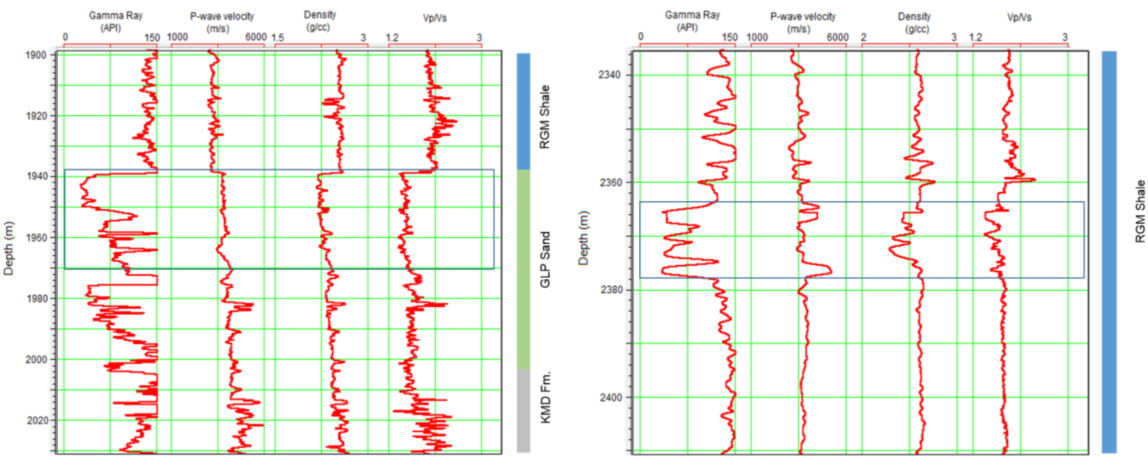

(a) For well KE (b) For well KR

Fig. 2 Log data from (a) well KE at Endamuru; and (b) well KR at Suryaraopeta fields. The reservoir zones are marked. RGM, Raghavapuram, GLP, Gollapalli, KMG, Kommugudem

bearing zones are shown in Fig. 2. Fig. 2(a) from well KE shows the clean sand reservoir with low *Vp*/*Vs*, low density and low gamma ray. Fig. 2(b) from well KR indicates shaly sand reservoir with low *Vp*/*Vs*, low density and alternate high-low gamma responses. Shale lamina produces relatively

Table 1 Estimation of Petrophysical Parameters from selected depth intervals of two wells in K-G basin

Wells	Hydrocarbon bearing zone		Petrophysical parameter			Formation	Geological age
	Depth interval (m)	Thickness (m)	*Vsh* (%)	Effective porosity (%)	Water saturation (%)		
KE	1939-1958	19	2	14	10	Gollapalli sandstone	Early cretaceous
	1959-1964	5	3	15	27		
KR	2365-2368	3	15	15	20	Raghavapuram shale	Early cretaceous
	2370-2374	4	17	19	22		

high gamma responses within shaly sand reservoir. The reservoir sandstones in well KE and KR are part of the Gollapalli Sandstone and Raghavapuram Shale formations of Early Cretaceous age, deposited under shallow marine environment. These reservoirs with water saturation (*Sw*) varying from 10 to 27% are examples of cemented reservoirs with effective porosity (φ_e) ranging from 14 to 19% and shale volume (*Vsh*) varying from 3% in clean sand reservoir to 17% in shaly sand reservoir (Table 1).

3. Rock mechanical properties from well logs

The rock mechanical parameters for two wells: KE and KR are computed from sonic logs of *Vp* and *Vs*. The unconfined compressive strength (UCS), elastic moduli such as: shear modulus (*G*), Young's modulus (*Y*), bulk modulus (*K*) and Poisson's ratio (σ) have been estimated from velocity of *P* wave (*Vp*), and velocity of S wave (*Vs*) and density (ρ) log data using the equations provided by (Mohammed and Zillur 2001, Potter and Foltinek 1997)

Poisson's ratio, $$\sigma = \frac{1}{2}\frac{\left((V_p/V_s)^2-2\right)}{\left((V_p/V_s)^2-1\right)} \quad \text{(a)}$$

Shear modulus, $$G = V_s^2 \rho \quad \text{(b)}$$

Young's modulus, $$Y = 2 * G(1 + \sigma) \quad \text{(c)}$$

Bulk modulus, $$K = \rho * \left(V_p^2 - \frac{4}{3}V_s^2\right) \quad \text{(d)}$$

And Cohesive Strength (S_0)

$$S_0 = 0.025 * 10^{-9}\frac{Y}{K}[0.008 * Vsh + 0.0045(1 - Vsh)] \quad \text{(e)}$$

where *Vsh* is the volume of shale.

Unconfined Compressive Strength is therefore

$$UCS = \frac{S_0}{0.289} \quad \text{(f)}$$

The values of *G*, *Y*, *K* and UCS in Raghavapuram Shale are increased in the Gollapalli

Sandstone followed by the increase in sediments of Kommugudem Formation (Fig. 3). The value of σ varies from 0.32 to 0.47 in Raghavapuram Shale with lowering of its value upto 0.12 in

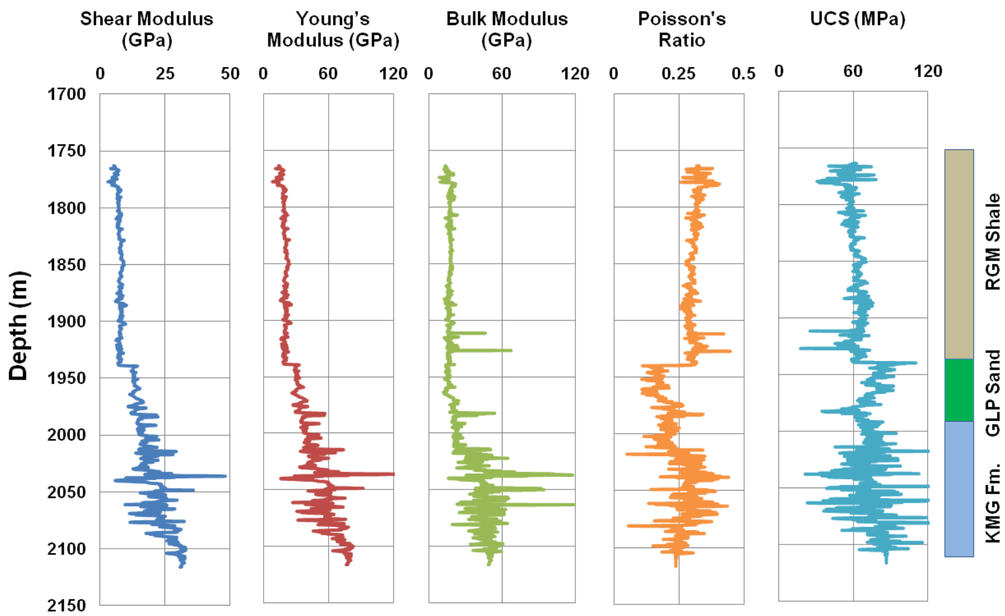

(a)

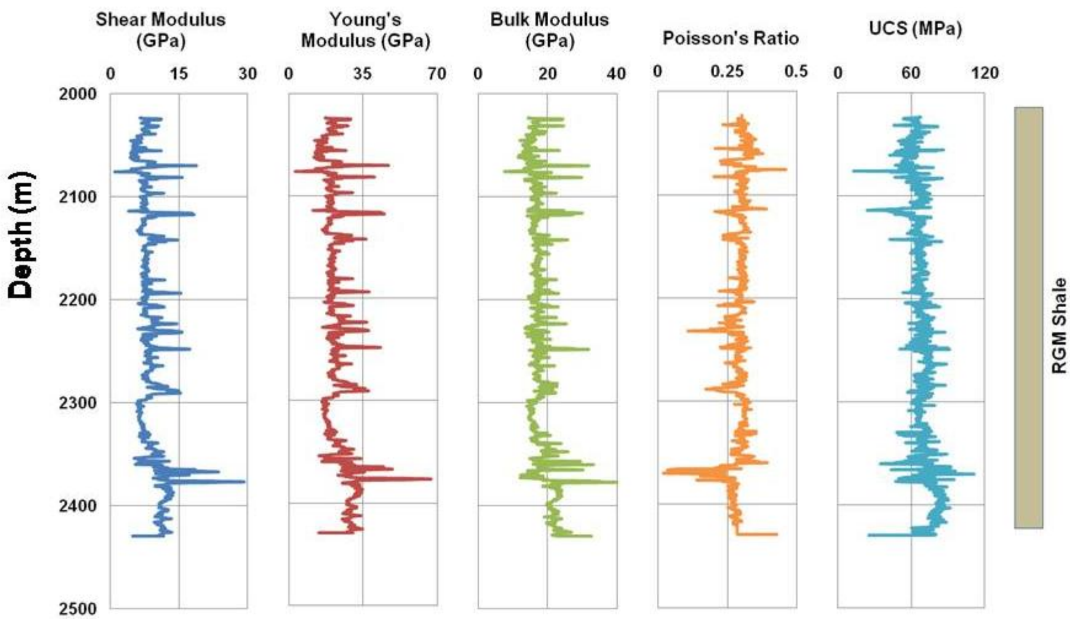

(b)

Fig. 3 Illustrates the rock mechanical parameters computed for available depth interval in well (a) for KE; and (b) for KR. The lithology are also shown in colour column beside each plots. RGM, Raghavapuram, GLP, Gollapalli and KMG, Kommugudem, Fm., Formation

Gollapalli Sandstone Formation and further increase in Kommugudem Formation. Gas producing zone is characterized by low Poisson's ratio between depths 1939 m and 1958 m in Gollapalli Sandstone Formation.

4. Rock physics model

Fig. 4 illustrates the flowchart showing the steps of rock physics diagnostic (RPD) modeling and RPT analysis for sand reservoirs in the K-G basin. The models: friable sand, constant cement and contact cement for specific target zones of two wells (Fig. 2) have been used to link elastic and seismic properties with geologic properties and to estimate the extent to which these geologic trends may influence the lithology and fluid sensitivity of the seismic parameters. Here we employ the modified HS bounds using the HM theory. An attempt has been given on deriving models for clean sands, shaly sands and shales as these are the lithologies encountered in two wells under the study area. The methodologies of RPD modeling and RPT analysis are as following:

(a) Using HS and HM theory to define bounds, we model the given lithology under investigation by first defining end-members. The low porosity end member is at 0% porosity indicates the mineral point. Pressure dependent HM theory is used to estimate the dry moduli of the rock at critical porosity (0.40) end member. Then, we have constructed moduli of the solid mineral for zero porosity
(b) The moduli of the dry rock between critical porosity and zero porosity are estimated by HS bounds, which provide theoretical approximations of effective elastic moduli of a mixture of grains and pores under given pressure conditions for the given lithology. HS bounds assume that each component and the rock are isotropic and elastic.
(c) We superimpose the rock physics models on in situ data from wells using cross plots to estimate the moduli and velocities that would be needed to match the reservoir sandstone and cap rock shale data.
(d) We attempt an estimate about the mineralogical composition of the sandstone and shales and also the possible geologic trends.

The elastic bulk moduli of brine and gas saturated rocks are calculated to observe the effect of fluid substitution. The dry rock properties calculated from the combined HM and HS bounds are used as the inputs into Gassmann's equation to compute the saturated rock properties assuming uniform saturation. Fluid substitution is performed by using Gassmann's relations (Gassmann 1951a, b) to investigate the lithology and fluid sensitivity of elastic and seismic parameters under various conditions such as pressure, temperature, mixed saturations, gas-oil-ratio (GOR), brine salinity. From these, *P*- and *S*-wave velocity and density of brine or gas saturated rocks have been calculated.

(e) Finally *Vp*/*Vs* vs. *P*-impedance (AI) has been computed so that a cross plot of *Vp*/*Vs* against AI can be generated. The simplest work flow and summary is as follows in Fig. 3.

Rock properties like velocity and bulk density, are a function of various diagenetic compaction processes in sedimentary rocks Avseth *et al*. (2005). Reservoir characterization, basin modeling and seismic interpretation require information on rock properties. This may be obtained from well log data, experimental compaction and petrographic analysis of core samples Marcussen *et al*. (2010). Quartz cementation is the most important process controlling reservoir quality in deeply

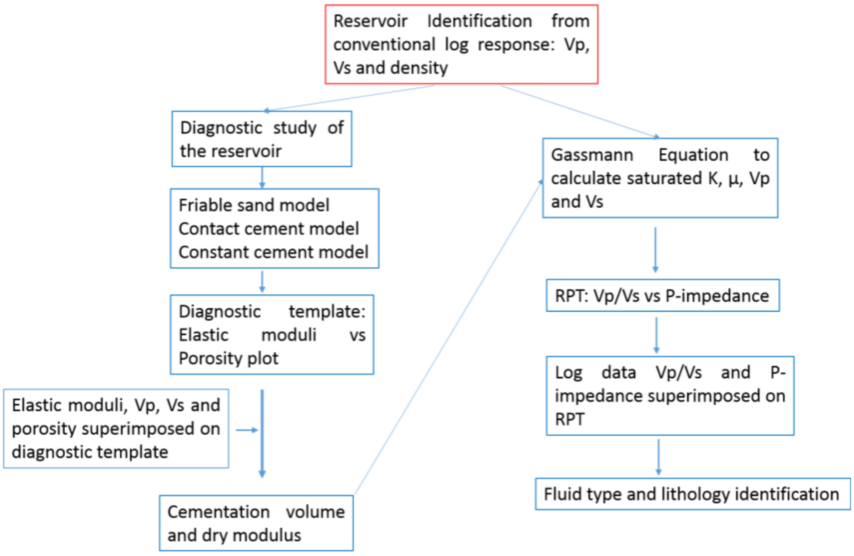

Fig. 4 Flowchart indicating the steps followed in rock physics diagnostic and RPT generation for sand reservoir in K-G basin

buried, quartz-rich sandstones e.g., Walderhaug and Bjørkum (2003). Hossain and Macgregor (2014) demonstrate rock physics diagnostic analysis to describe the functional relationship between seismic velocity and porosity, which is consistent with local geology, characterizing diagenetic pore-filling cement and contact cements.

5. Rock physics diagnostics

To build a rock physics model, various velocity-porosity trends are to be obtained from the entire volume of data and these separate trends are assigned to appropriate depth intervals and depositional sequences. This procedure is called rock physics diagnostic. Rock physics diagnostic is typically conducted on well log and core data Avseth *et al*. (2000). It describes the texture of rock: the position of diagenetic cement; grain size sorting; effect of clay, etc. Generally, *P* and *S*-wave velocities are not considered as the best fluid indicator due to the coupling effect between *P* and *S*-waves through the shear modulus and bulk density. Rock physics trends appear more discretely in the modulus-porosity plane than in the velocity-porosity plane Durrani *et al*. (2014). Bulk modulus shows sensitivity to pore fluid (water) and deformation produced by a seismic wave resulting in change of pore volume. Shear modulus is not affected by different fluids. The work space for rock physics analysis is the rock physics plane that may be (a) velocity-porosity; (b) impedance-porosity; and/or (c) modulus-porosity plane. Primarily we prefer elastic moduli-porosity planes to correlate change of fluid effect in bulk modulus in comparison with velocity-porosity planes for diagnosing rocks. In this study, *P*-wave velocity, bulk and shear moduli as a function of porosity from wells KE and KR are superimposed on the combinations of three models such as: friable sand model Dvorkin and Nur (1996), the contact cement model Dvorkin *et al*. (1994) and the constant cement model Avseth *et al*. (2005). These diagnostic models with prior knowledge on cement quantification from thin section studies are helpful for prediction of constant cement model with cement percentages, which in turn will be used for finding coordination number in the HM theory to construct dry modulus of rock at critical porosity for RPT development. Since we do not have quartz cement quantity from thin section studies, hence the models proposed by Avseth *et al*. (2005) are used for cement quantification for RPT generation in this basin.

Quantification of cement is created to fit the well log data in velocity-porosity and rock moduli-porosity templates. HM theory and lower HS bound are used to describe the friable sand model. For cemented sand, the upper HS bound is utilized. In general, elastic properties of rocks are controlled by lithology (composition and texture), porosity (amount and type), pore fluids, depth (differential pressure, temperature, age and lithification), frequency, anisotropy. These controlling parameters usually are different in various geological environments. The reservoirs occurring in the Gollapalli Sandstone of the Late Jurassic–Early Cretaceous and Raghavapuram Shale of Early Cretaceous age represents shallow marine environment of deposition (Prasad 1999, Murthy *et al*. 2011). HM contact theory Mindlin (1949) is used firstly to construct dry modulus of rock at the high porosity usually called critical porosity. For sand, the critical porosity is taken as 40%. Dry elastic moduli at high porosity are given by Dvorkin *et al*. (1996).

$$K_{HM} = \left[\frac{n^2(1-\emptyset_C)^2\mu^2}{18\pi^2(1-\vartheta)^2}P\right]^{\frac{1}{3}} \quad (1)$$

$$\mu_{HM} = \frac{5-4\vartheta}{5(2-\vartheta)}\left[\frac{3n^2(1-\emptyset_c)^2\mu^2}{2\pi^2(1-\vartheta)^2}P\right]^{\frac{1}{3}} \quad (2)$$

where, K_{HM}, μ_{HM} = dry rock bulk and shear moduli, respectively, at critical porosity $\emptyset_C$; n = coordination number; P = net confining pressure, which is equal to effective pressure (assumes Biot coefficient is equal to one); μ = shear modulus for solid phase (mineral modulus); ϑ = Poisson's ratio for solid phase. Coordination number (average number of contacts per grain) increases with decreasing porosity, which is the result of more efficient packing under increasing confining pressure Mavko *et al*. (2009). Shales with high porosity have relatively small coordination number, and vice versa. Coordination numbers for cemented sand reservoir and shale are assumed as 8.69 and 3.37 respectively.

Rock physics models are dealing with the elastic properties of rock. Rock as a composite is made of two basic elements: the mineral frame and the pore fluid. The mineral frame includes more than one mineral. A traditional treatment of this situation is to analytically create a single, or "effective," mineral whose elastic properties depend on those of the mineral constituents, which can be used to calculate the elastic properties of the dry mineral frame. Hypothetical effective mineral known as "effective solid phase" is a composite itself, made of several pure-mineral elastic components with known volumetric fractions. There are the upper and lower bounds for the bulk and shear moduli of this elastic composite Mavko *et al*. (2009). Dry rock elastic moduli can be estimated based on the Hashin-Shtrikman (Hashin and Shtrikman 1963) bounds between the high porosity and zero porosity. Elastic moduli and density of different constituents of dry solid matrix such as: quartz, feldspar and clay are tabulated in Table 2 for computation of dry elastic moduli with HS bounds for wells in K-G basin.

The HS bounds provide the narrowest range of elastic moduli without specifying geometries of constituents Mavko *et al*. (1998, 2009)

$$K_{HS\pm} = K_1 + \frac{f_2}{(K_2 - K_1)^{-1} + f_1\left(K_1 + \frac{4}{3}\mu_1\right)^{-1}} \tag{3}$$

$$\mu_{HS\pm} = \mu_1 + \frac{f_2}{(\mu_2 - \mu_1)^{-1} + \frac{2f_1(K_1 + 2\mu_1)}{5\mu_1\left(K_1 + \frac{4}{3}\mu_1\right)}} \tag{4}$$

K_{HS}, μ_{HS} = bulk and shear moduli calculated using HS bounds
K, μ = bulk and shear mineral moduli of different constituents
(index refers to individual phase 1 or 2)
f = volume fraction of individual phases.

The upper bound is usually used for cemented rocks (stiffest material is subscribed 1), and the lower bound for unconsolidated sands (softest material is subscribed 1). For the modeling purposes in this work a modified HS upper bound has been used. It connects two end members (high porosity and zero porosity) in the porosity-moduli plane i.e., the mineral point and the critical porosity point are connected by the unconsolidated line, which is the modified lower HS bound Dvorkin and Nur (1996).

The behavior of *P*-wave velocity and elastic moduli (bulk and shear moduli) with porosity due to cementation are captured by contact cement and constant cement models. In well KE, a thick sand interval (Fig. 2(a)) is marked by low and varying gamma ray readings as well as high velocity (about 3.7 to 4 km/s). This sand layer is surrounded by shale whose gamma ray and velocity contrast those of the reservoir sand. In well KR, we observe alternate variation of gamma ray response between clean sand and shale (Fig. 2(b)) in reservoir zone. The clean sand and shaly sand reservoir zones in both wells represent the same stratigraphic unit, although located at different depths and in separate gas fields. Gollapalli Sandstone and Raghavapuram Shale formations in two wells are comprised of shale, both friable sands and cemented sandstones. The stiffness of rock depends not only on porosity and mineralogy but also on the rock's microstructure (texture), i.e., the arrangement of the components of the solid phase at the pore scale. P-wave velocity is plotted versus porosity for sands appreciating the influence of microstructures. The cement model assumes that porosity decreases from the initial critical porosity value due to the uniform deposition of cement layers on the surface of the grains. The diagenetic cement dramatically increases the stiffness of the sand by reinforcing the grain contacts Durrani *et al*. (2014). For diagnostic purposes we crossplot the elastic properties from selected depth intervals of two wells (1939-1964 m of KE and 2364-2378 m of KR) in velocity-porosity and moduli-porosity planes superimposing theoretical rock physics models (Figs. 5-7). The cross plots show that gradually increasing cementation corresponds with increasing P-wave velocity and elastic moduli.The data from Gollapalli Sandstone formation of well KE is sorted into two parts: sands with more amounts of quartz cement at grain contacts and sands from the Gollapalli Sandstone with 2-6% cement. A large part of the scatter is observed in velocity-porosity and elastic moduli-porosity cross plots for KR well. This scattered effect is due to the clay existing in the Raghavapuram Shale. The data from Raghavapuram Shale formation of well KR is sorted into three parts: uncemented sand/friable sand, sands with more amounts of quartz cement at grain contacts and sands with 2-6% cement. The upper curve corresponds to the pure quartz cases while lower curve is for uncemented rock (Figs. 5-7). Data points falling on the upper curve of velocity-porosity plane represent all

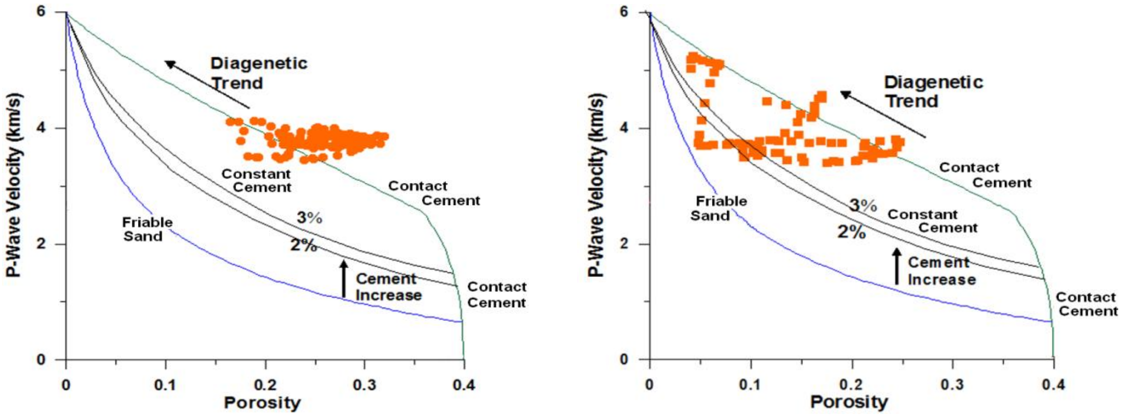

(a) For well KE (b) For well KR

Fig. 5 Rock Diagnostic Plot between *P*-wave velocity and Porosity of reservoir sands for using constant cement, contact cement and friable sand model (after Dvorkin and Nur 1996, Avseth *et al*. 2000, 2005)

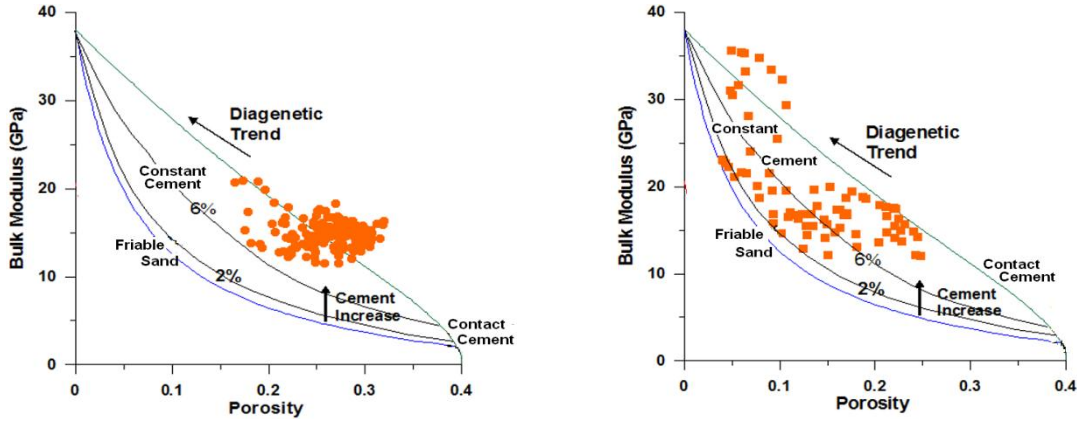

(a) For well KE (b) For well KR

Fig. 6 Rock Diagnostic Plot between Bulk modulus and Porosity of reservoir sands using constant cement, contact cement and friable sand model (after Dvorkin and Nur 1996, Avseth *et al*. 2000, 2005)

cement deposited precisely at grain contacts and slope flat for well KE and slope steep for well KR. Data points falling between the constant cement lines correspond to the uniform deposition of cement on grain surfaces. The data points falling on the upper curve of bulk modulus-porosity plane are at grain contacts and steep slope for both wells. The points of elastic moduli-porosity plane falling between the constant cement lines are also in gentle slope to steep slope. It is quite possible that the variation in microcracks may be the major reason for difference or variation of slope between velocity-porosity and moduli-porosity planes. It is noticed that the maximum data points fall on the constant cement line (6%) representing uniformly deposited cement on grain surface. The reservoir zones identified in the depth intervals; 1939-1964 m of KE and 2364-2378 m of KR wells are characterized by the constant cement model as noticed from Figs. 4, 5 and 6. The distributions of points in these RPD plots indicate different geological trends showing lower

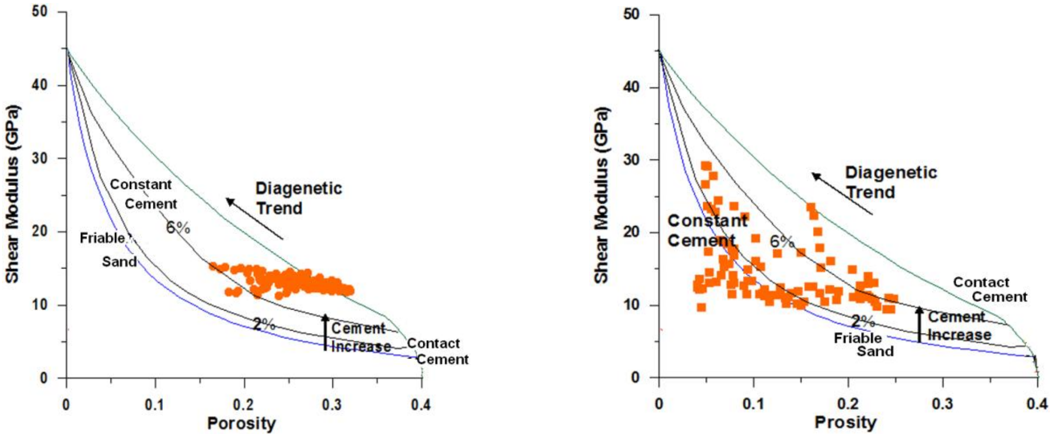

(a) For well KE (b) For well KR

Fig. 7 Rock Diagnostic Plot between Shear Modulus and Porosity of reservoir sands using constant cement, contact cement and friable sand model (after Dvorkin and Nur 1996, Avseth *et al*. 2000, 2005)

to higher porosity value. Gas saturated pay zone sand produce distinctive and separate velocity-porosity and elastic moduli-porosity trends for two wells. High cementation of more than 6% is observed in Gollapalli sand reservoir in well KE. The friable sand as well as cemented sand with varying cementation of 2 to more than 6% are observed in well KR. Comparing these three RPD models, constant cement to contact cement model are considered to analyse rock texture and dry rock modulus of reservoirs of both of wells.

6. Rock physics template

Next step is fluid substitution i.e., to compute elastic moduli of saturated porous rock with fluid (brine or hydrocarbon). Gassmann's equation has been applied to estimate the fluid substitution effect in a RPT and elastic modulusat the desired saturation Gassmann (1951a, b). Biot-Gassmann fluid substitution model (Gassmann 1951a, b, Biot 1956) is used for estimation of saturated elastic modulus of reservoir sandsfrom dry modulus with varying water saturation, and for porosities from zero to critical porosity, and is expressed as

$$K_{Sat} = K_{Dry} + \frac{\left(1 - \frac{K_{Dry}}{K_{Mineral}}\right)^2}{\frac{\emptyset}{K_{Fluid}} + \frac{1-\emptyset}{K_{Mineral}} - \frac{K_{Dry}}{K_{Mineral}}} \tag{5}$$

where K_{Sat} = Saturated bulk modulus, K_{Dry} = dry bulk modulus, K_{Fluid} = fluid bulk modulus $K_{Mineral}$ = bulk modulus of mineral

Since the shear modulus of the fluid is zero, the shear modulus of the fluid saturated rock is given by

$$\mu_{Sat} = \mu_{Dry} \tag{6}$$

And the bulk density of the fluid saturated rock (ρ_b) is given by

$$\rho_b = \rho_g(1-\emptyset) + \rho_{fl}\emptyset \quad (7)$$

Where ρ_q density of gas and ρ_{fl} = density of fluid.

The bulk modulus of the "effective" fluid phase can be computed like the solid phase. The components of which may include water, oil, and gas. If all individual fluid phases remain in perfect hydraulic communication, that is, the pressure in the gas is the same as in the oil and the same as in the water, the effective bulk modulus of such an immiscible system (K_{Fluid_av}) is expressed as Domenico (1976)

$$\frac{1}{K_{Fluid\_av}} = \frac{S_{br}}{K_{br}} + \frac{S_{oil}}{K_{oil}} + \frac{S_{gas}}{K_{gas}} \quad (8)$$

where K_{Fluid_av} = effective fluid bulk modulus, K_{br} = brine bulk modulus, K_{oil} = oil Bulk modulus and K_{gas} = gas bulk modulus, S_{br} = brine saturation, S_{oil} = oil saturation and S_{gas} = gas saturation.

Bulk density of rock also changes with the pore fluid densities as given in equation (7). Therefore, fluid density (ρ_{fl}, density of fluid mixture say water and hydrocarbon) is defined as

$$\rho_{fl} = S_w\rho_w + (1-S_w)\rho_{hc} \quad (9)$$

where S_w = water saturation, ρ_w = water density and ρ_{hc} = hydrocarbon density.

And the fluid modulus (K_{fl}) is given by Wood (1941)

$$K_{fl} = \left(\frac{S_w}{K_w} + \frac{(1-S_w)}{K_{hc}}\right) \quad (10)$$

where K_w = water bulk modulus and K_{hc} = hydrocarbon modulus.

Fluid substitution is required to know K_{sat} and the *P*-wave and *S*-wave velocities are then finally computed using following equations as

$$V_P = \sqrt{\frac{K_{sat} + \mu}{\rho_b}} \quad (11)$$

$$V_S = \sqrt{\frac{\mu}{\rho_b}} \quad (12)$$

Geological constraints on RPT include lithology, mineralogy, burial depth, diagenesis (cementation), pressure and temperature from well log, core sample and well testing data. The common form of template, *Vp*/*Vs* vs. AI is serving as good indicator of lithology and fluid indicator (e.g., Avseth *et al*. 2005, Xin and Han 2009). We have used mineral contents, lithology, coordination number, pressure and temperature from reservoirs occurring in Gollapalli Sandstone and Raghavapuram Shale from previous study and personal contact with Oil and Natural Gas Corporation Ltd. (Chatterjee and Mukhopadhyay 2002, Singha and Chatterjee 2014, Singha *et al*. 2014). The average modulus of mineral mixture (quartz, feldspar and clay) is given by the Voigt-Reuss-Hill average or simply VRH average Mavko *et al*. (2009) of sand grain for the reservoirs in the K-G basin is given below:

Table 2 Elastic moduli and density of minerals assumed for RPT (Mavko *et al*. 2009, Avseth 2000)

Minerals	Bulk modulus (GPa)	Shear modulus (GPa)	Density (g/cc)
Quartz	36.6	45.0	2.65
Feldspar	75.6	25.6	2.60
Clay	20.9	6.9	2.58

Table 3A Reservoir parameters for RPT

Parameters	Value
Pressure	3370.0 Psi
Gas gravity	0.6 API
Temperature	117.05^{0}C
Oil gravity	51.3 API
Gas-oil ratio	100 L/L
Salinity	38610 ppm

Table 3B Fluid Properties used for Gassmann-Biot modelling

Fluid type	Bulk modulus (GPa)	Density (g/cc)
Gas	0.0478	0.1291
Oil	0.4558	0.6581
Brine Water	0.9853	0.9853

Bulk Modulus: 30.0 GPa, Shear Modulus: 26.61 GPa and Density: 2.51 g/cc

Pore fluids strongly influence the seismic properties. Their properties, particularly bulk moduli, densities, viscosities and velocities vary with composition, pressure and temperature. Batzle and Wang (1992) derived a set of relations, using a combination of thermodynamic relations, empirical trends, to explain the effects of pressure, temperature and composition on the properties of hydrocarbon gases and oils and of brines. Tables 3A and 3B lists the reservoir parameters and calculated fluid properties at specified pressure and temperature for well KE. The RPT is calibrated using the well logs at KE well.

In general for most mineral the sum of the pure shear elastic moduli (*c*) is equal to the sum of the off-diagonal shear moduli (*b*). In quartz the ratio of b/c is 0.2 instead of 1 and Poisson's ratio of quartz is 0.056 (Levien *et al*. 1980). This value of b/c reflects the expanding or contracting spirals of tetrahedral crystal structure of quartz causing the higher shear modulus of quartz than its bulk modulus.

The bulk modulus and density for different fluids as tabulated in Table 3b are used in Gassmann fluid substitution modeling. From calculated moduli and density at new saturation, *Vp* and *Vs* are determined and *Vp*/*Vs* vs. AI template is created. The resulting rock physics model for sands and shales, with log data from 1920-to 2010 m of KE and 2340-2429 m of KR wells are superimposed, in this *Vp*/*Vs* vs. AI template, color coded by gamma ray (Figs. 8 and 9). Two trend lines present shale and sand line. Modeled shale porosity range from 5-65%, and modeled sand porosity 0-35%. Each of porosity sand lines has its saturation line, which starts as 100% brine

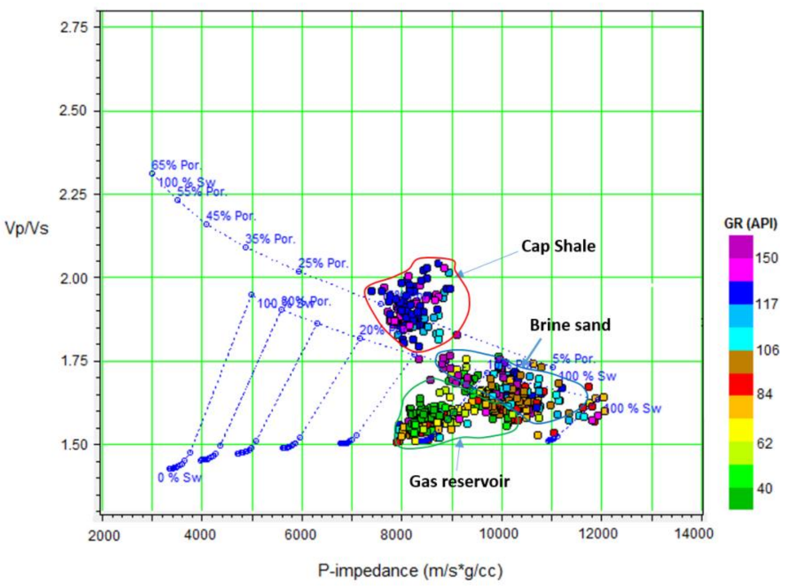

Fig. 8 The RPT posted in the crossplot of *Vp*/*Vs*. vs. *P*-impedance calculated from well log data of well KE at Endamuru field. Gas sand, brine sand and cap shale are identified

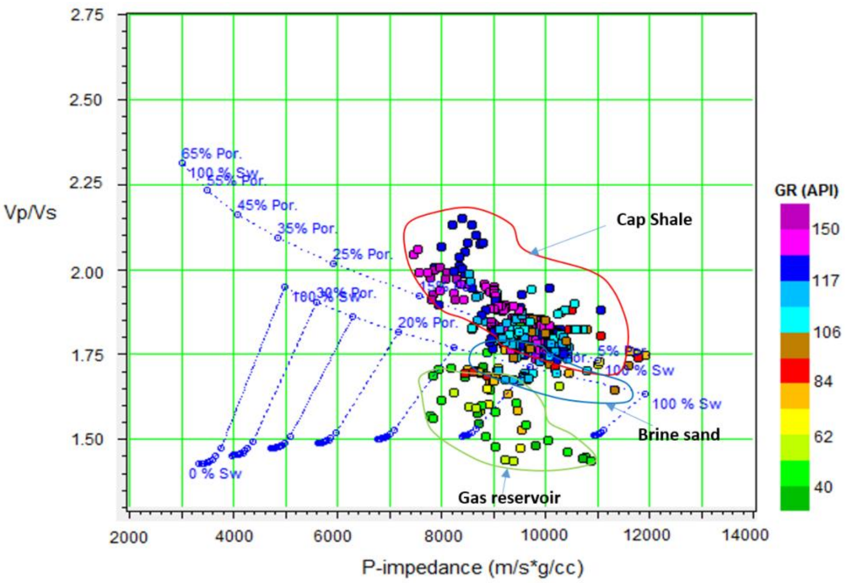

Fig. 9 The RPT posted in the crossplot of *Vp*/*Vs*. vs. *P*-impedance calculated from well log data of well KR at Suryaraopeta field. Gas sand, brine sand and cap shale are identified

saturated sand, and end as gas saturated. Figs. 8 and 9 includes a background shale-trend line, a brine-sand-trend line, and curves for increasing gas saturation as a function of porosity on a rock physics template in *Vp*/*Vs* vs. AI cross-plot domain. This template is able to identify cap rock i.e., shale, brine sand and gas sand reservoirs for these two wells.

7. Gas sand detection from neutron vs. density cross plot

Various rock physics models have their own benefits and limitations Avseth *et al*. (2010). Fluid and lithology discrimination are carried out for seismic reservoir characterization by applying *Vp*/*Vs* vs. AI RPT. Data points concentrate within a narrow zone indicating high AI and *Vp*/*Vs* ratio suggest that application of rock physics template in the study area needs significant modification compared to generalized RPTs. As typically used in the oil and gas industry, the term rock physics is usually applied to the measurement, modeling and interpretation of elastic wave propagation in sedimentary rocks Bello *et al*. (2015). RPD modeling and RPT have been used to identify productive sands from seismic away from well control. Conventional log responses in well KE and KR have suggested the presence of sand/shaly sand reservoir in these wells. The high resistivity values are noticed along with low gamma ray and cross over between neutron and density logs (Fig. 10). This section presents identification of gas bearing zones from neutron and density cross plots. The wells exhibit a dominantly shale/sand/shale sequence. The wells have been analysed in terms of fluid type and lithology. Shale lithologies have been delineated by the high gamma ray value. Shale lithologies cause the deflection of resistivity to the far left due to its high conductive nature. Regions showing low gamma ray, high resistivity (100 to 300 ohm-m), and high acoustic impedance (8000 to 11000 gm/c.c * m/sec) are mapped as sand lithologies. Sand lithologies showing very high acoustic impedance and high resistivity are regions of high gas saturation. Total porosity of rocks (sand/shale lithology) is a function of grain size, packing, shape, sorting, intergranular matrix and cement. RPD modeling and RPT analysis have given access to know about the reservoir microstructure, cementation, fluid type and lithology under specified pressure and temperature conditions. The neutron and density cross plot for the selected depth interval 1932-1984 m of well KE (Fig. 11(a)) reveals the occurrence gas bearing sand of Gollapalli

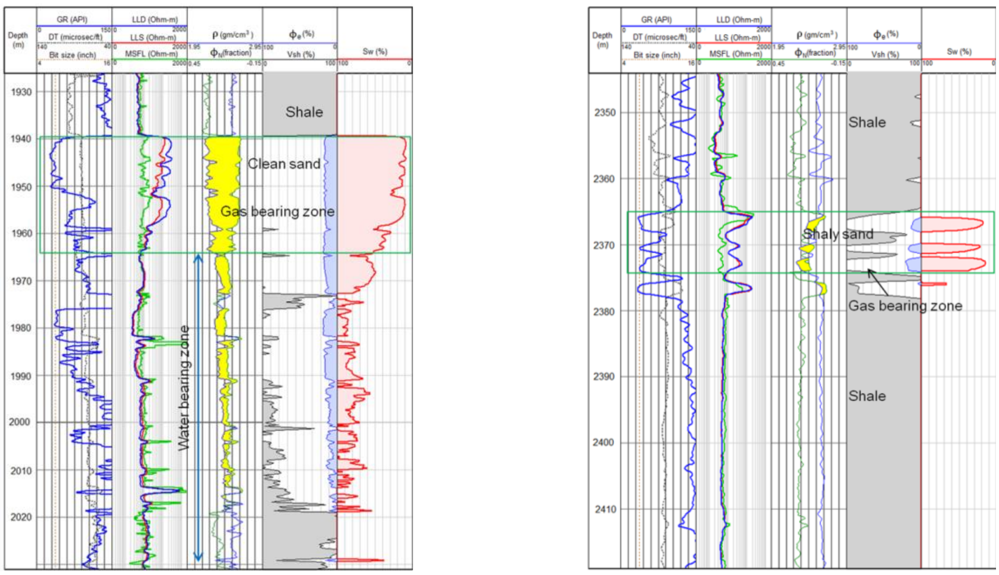

(a) for well KE (b) for well KR

Fig. 10 Conventional log responses indicating the gas bearing zones in the selected depth intervals in wells; Φ*n*, neutron porosity and *ρ*, density

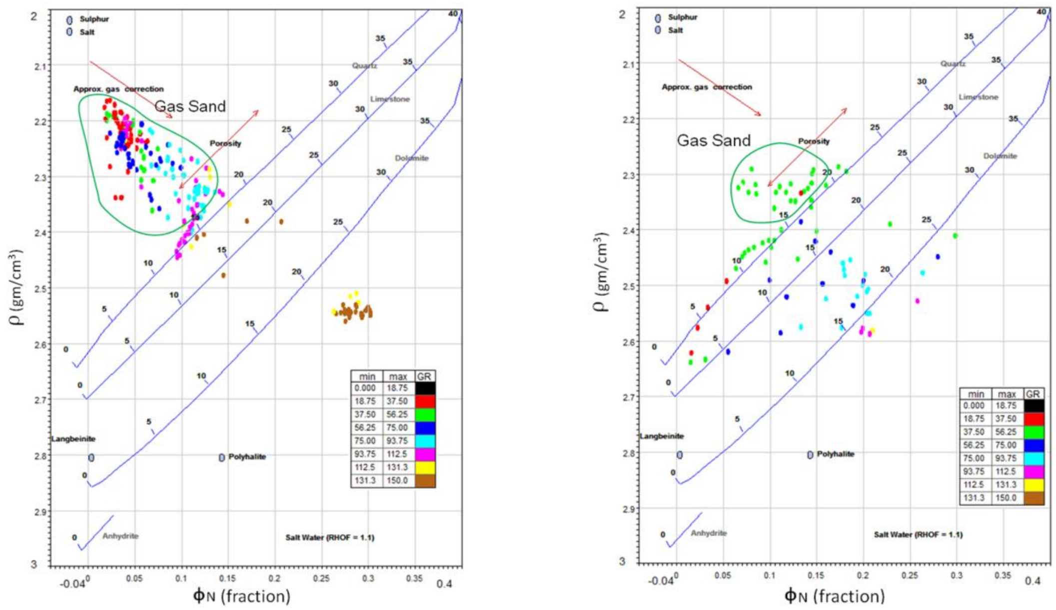

(a) for well KE (b) for well KR

Fig. 11 Cross plot between neutron porosity and density. Gas sands are identified for the selected depth intervals marked in Fig. 9. Φn, neutron porosity and ρ, density

formation. The cross plot shown in Fig. 11(b) for well KR within depth interval 2354-2389 m is affected by the presence of laminated shale in the Raghavapuram Shale formation. Clean gas bearing sand and shaly sand gas bearing zones are identified from log analysis (Fig. 10) as well as from neutron porosity vs. density cross plot (Fig. 11).Therefore log data posted on generated RPT are matched well with the conventional log data as observed in the cross over between neutron and density logs. The RPT analysis is more powerful technique for reservoir characterization in any geological environment. This could be used as a forecasting and risk minimizing for reservoir identification and local geological effect in the undrilled area.

8. Conclusions

Rock physics diagnostic models are used for cement quantification in constant cement model for reservoir zones from two wells. The contact cement line corresponds to the case where rock is formed by quartz-cement rims growing on sand grains. *P* wave velocity increases with slightly decreasing porosity in two wells. The friable sand line corresponds to the well KR indicates reduction of porosity due to loose pore-filling material such as small grains, mica and detrital clay particles. The generated RPT is posted on the cross plots of Vp/Vs vs. AI which are calculated from well logs. Even though the RPT is only calibrated using the well logs from KE well at Endamuru, it is applicable at KR well at Suryaraopeta field since these two areas have similar geological depositional environments. This template demonstrates the identification of gas sand reservoir, cap shale and brine sand for two wells. Rock physics models and RPT constrained by local geology in K-G basin can be used for prediction of lithology and hydrocarbons. RPT generated for the shallow marine environment is correctly indicating gas saturation with lithology as it is observed from conventional neutron-density cross plots. Thus, we can predict the lithology and fluid content at undrilled areas using the well logs of KE as a reference if we assume those areas have the similar geological deposition environment to Endamuru.

Acknowledgments

We thank Oil and Natural Gas Corporation (ONGC) Ltd. for permission to use the well log data to carry out research work. Data are available for academic purposes. The work is funded by Ministry of Earth Science through the R&D project MoES /P.O./(Seismo)/1(138) 2011 dated 9.11.12. Authors are also thankful to Department of Science and Technology (DST), India for Inspire Project.

References

Avseth, P. (2000), "Combining rock physics and sedimentology for seismic reservoir characterization of north sea turbidite systems", Ph.D. Thesis; Stanford University, Stanford, CA, USA .

Avseth, P., Dvorkin, J. and Mavko, G. (2000), "Rock physics diagnostic of north sea sands: link between microstructure and seismic properties", *Geophys. Res. Lett.*, **27**(17), 2761-2764.

Avseth, P., Mukerji, T. and Mavko, G. (2005), *Quantitative Seismic Interpretation: Applying Rock Physics to Reduce Interpretation Risk*, Cambridge University Press, Cambridge, UK, 359 p.

Avseth, P., Jørstad, A., Wijngaarden, A.J. and Mavko, G. (2009), "Rock physics estimation of cement volume, sorting, and net-to-gross in north sea sandstones", *The Leading Edge*, **28**(1), 98-108.

Avseth, P., Mukerji, T., Mavko, G. and Dvorkin, J. (2010), "Rock physics diagnostics of depositional texture, diagenetic alterations, and reservoir homogeneity in high porosity siliciclastic sediments and rocks – A review of selected models and suggested work flows", *Geophysics*, **75**(5), A31-A47.

Batzle, M. and Wang, Z. (1992), "Seismic properties of pore fluids", *Geophysics*, **57**(11), 1396-1408.

Bello, R., Igwenagu, C.L. and Onifade, Y. (2015), "Cross plotting of rock properties for fluid and lithology discrimination using well data in a Niger Delta Oil Field", *J. Appl. Sci. Environ. Manage.*, **19**(3), 539-546.

Biot, M.A. (1956), "Theory of propagation of elastic waves in a fluid-saturated porous solid. I. Low-frequency range", *J. Acoust. Soc. Am.*, **28**(2), 168-191.

Chatterjee, R. and Mukhopadhyay, M. (2002), "Petrophysical and geomechanical properties of rocks from the oil fields of the Krishna-Godavari and Cauvery Basins, India", *Bull. Eng. Geol. Environ.*, **61**(2), 169-178.

Chatterjee, R., Datta Gupta, S. and Farooqui, M.Y. (2013), "Reservoir identification using full stack seismic inversion technique: A case study from Cambay basin oilfields, India", *J. Petrol. Sci. Eng.*, **109**, 87-95.

Datta Gupta, S., Chatterjee, R. and Farooqui, M.Y. (2012), "Rock physics template (RPT) analysis of well logs and seismic data for lithology and fluid classification in Cambay basin", *Int. J. Earth Sci.*, **101**(5), 1407-1426.

Domenico, S.N. (1976), "Effect of brine-gas mixture on velocity in an unconsolidated sand reservoir", *Geophysics*, **41**(5), 882-894.

Durrani, M.Z.A., Willson, K., Chen, J., Tapp, B. and Akram, J. (2014), "Rational rock physics for improved velocity prediction and reservoir properties estimation for granite wash (tight sands) in Anadarko Basin, Texas", *Int. J. Geophys.*, Article ID 209351, 1-15.

Dvorkin, J. and Nur, A. (1996), "Elasticity of high-porosity sandstones: Theory for two North Sea data sets", *Geophysics*, **61**(5), 1363-1370.

Dvorkin, J., Nur, A. and Yin, H. (1994), "Effective properties of cemented granular material", *Mech. Mater.*, **18**(4), 351-366

Dvorkin, J., Nur, A. and Chaika, C. (1996), "Stress sensitivity of sandstones", *Geophysics*, **61**(2), 444-455.

Gassmann, F. (1951a), “Elastic waves through a packing of spheres”, *Geophysics*, **16**(4), 673-685.

Gassmann, F. (1951b), “Elasticity of porous media”, *Uber die elastizitatporosermedien*, *Vierteljahrsschrift der Natur forschenden Gesselschaft*, **96**, 1-23.

Gray, D., Day, S. and Schapper, S. (2015), “Rock physics driven seismic data processing for the athabasca oil sands northeastern Alberta”, *CSEG Recorder*, March, pp. 32-40.

Gupta, S.K. (2006), “Basin architecture and petroleum system of Krishna Godavari Basin, east coast of India”, *Leading Edge*, **25**(7), 830-837.

Hashin. Z. and Shtrikman, S. (1963), “A variational approach to the elastic behavior of multiphase materials”, *J. Mech. Phys. Solids*, **11**, 127-140.

Hossain, Z and Macgregor, L. (2014), “Advanced rock-physics diagnostic analysis: A new method for cement quantification”, *The Leading Edge*, **33**(3), 310-316.

Levien, L., Prewitt, C.T. and Weidner, D.J. (1980), “Structure and elastic properties of quartz at pressure”, *Am. Minerol.*, **65**(9-10), 920-930.

Marcussen, Ø., Maast, T.E., Mondol, N.H., Jahren, J. and Bjørlykke, K. (2010), “Changes in physical properties of a reservoir sandstone as a function of burial depth – The etive formation, northern North Sea”, *Marine Petrol. Geol.*, **27**(8), 1725-1735.

Mavko, G., Mukerji, T. and Dvorkin, J. (1998), *The Rock Physics Handbook*: *Tools for Seismic Analysis in Porous Media*, Cambridge University Press, Cambridge, UK, 329 p.

Mavko, G., Mukerji, T. and Dvorkin, J. (2009), *The Rock Physics Hand Book*: *Tools for Seismic Analysis for Porous Media*, (2nd Eds.), Cambridge University Press, Cambridge, UK, 524.

Mindlin, R.D. (1949), “Compliance of elastic bodies in contact”, *J. Appl. Mech.*, **16**, 259-268.

Mohammed, Y.A. and Zillur, R. (2001), “A mathematical algorithm for modeling geomechanical rock properties of the Khuff and Pre-Khuff Reservoirs in Ghawar Field”, *SPE Middle East Oil Show*, Bahrain, March, Paper ID SPE 68194.

Murthy, M.V.K., Padhy, P.K. and Prasad, D.N. (2011), “Mesozoic hydrogeologic systems and hydrocarbon habitat, Mandapeta-Endamuru area, Krishna Godavari Basin India”, *AAPG Bulletin*, **95**(1), 147-167.

Mukerji, T., Avseth, P., Mavko, G., Takahashi, I. and Gonzalez, F. (2001), “Statistical rock physics: Combining rock physics, information theory, and geostatistics to reduce uncertainty in seismic reservoir characterization”, *The Leading Edge*, **20**(3), 313-319.

Omudu, L.M., Ebeniro, J.O., Xynogalas, M., Osayande, N. and Olotu, S. (2008), “Fluid discrimination and reservoir characterization from onshore Niger Delta”, *Proceedings of 78th Society of Exploration Geophysicists International Exposition and Annual Meeting*, Las Vegas, NV, USA, November, Volume 4, pp. 1996-2000.

Potter, C.C. and Foltinek, D.S. (1997), “Formation elastic parameters by deriving S-wave velocity logs”, CREWES Report; Volume 9, February.

Prasad, B. (1999), “Palynological characterisation, bio stratigraphy and depositional environment of Pre Tertiary litho-units of Krishna-Godavari basin, India”, *Geosci. J.*, **20**(2), 12-33.

Rao, G.N. (2001), “Sedimentation, stratigraphy, and petroleum potential of Krishna-Godavari basin, East Coast of India”, *AAPG Bull*etin, **85**(9), 1623-1043.

Samantaray, S. and Gupta, P. (2008), “An interpretative approach for gas zone identification and lithology discrimination using derivatives of $\lambda*\rho$ and $\mu*\rho$ attributes”, *Proceedings of the 7th Biennial International Conference and Exposition on Petroleum Geophysics*, Hyderabad, India, January, 386-341.

Sarasty, J.J. and Stewart, R.R. (2003), “Analysis of well-log data from the white rose oilfield, offshore Newfoundland”, *CREWES Research Report*, **15**, 1-16.

Sastri, V., Sinha, R.N., Singh, G. and Murti, K.V.S. (1973), “Stratigraphy and tectonics of sedimentary basins on ~~the~~ east coast of peninsular India”, *AAPG Bulletin*, **57**(4), 655-678.

Sastri, V.V., Venkatachala, B.S. and Narayanan, V. (1981), “The evolution of the east coast of India”, *Palaeogeography*, *Palaeoclimatology*, *Palaeoecology*, **36**(1-2), 23-54.

Shanmugam, G., Srivastava, S.K. and Das, B. (2009), “Sandy debrites and tidalites of pliocene reservoir sands in upper-slope canyon environments, offshore Krishna-Godavari Basin (India): Implications”, *J. Sedim. Res.*, **79**(9), 736-756.

Singha, D.K. and Chatterjee, R. (2014), "Detection of overpressure zones and a statistical model for pore pressure estimation from well logs in the Krishna-Godavari Basin, India", *Geochem*. *Geophys*. *Geosyst*., **15**(4), 1009-1020.

Singha, D.K., Chatterjee, R., Sen, M.K. and Sain, K. (2014), "Pore pressure prediction in gas-hydrate bearing sediments of Krishna-Godavari Basin, India", *Marine Geol*. **357**, 1-11.

Walderhaug, O. and Bjørkum, P.A. (2003), "The effect of stylolite spacing in quartz cementation in the lower jurassic stø formation, Southern Barents Sea", *J*. *Sedim*. *Res*., **73**(2), 146-156.

Wood, A.B. (1941), *Textbook of Sound Being an Account of the Physics of Vibrations with Special Reference to Recent Theoretical and Technical Developments*, (2nd Eds.), G. Bell and Sons Ltd., London, UK, 578 p.

Xin, G. and Han, D. (2009), "Lithology and fluid differentiation using a rock physics template", *The Leading Edge*, **28**(1), 60-65.

CC